

Heat Transfer in an Eccentric Gas Gap Annulus

T.M. Kalter, M.A.J. van Limbeek and S. Vanapalli

University of Twente
Applied Thermal Sciences lab,
Faculty of Science and Technology, The Netherlands

ABSTRACT

Heat transfer in the annular region between two cylindrical surfaces is widely studied in the context of gas-gap heat switches operating at cryogenic temperatures. Using a similar working principle, a tissue snap freezer is developed where a vial is cooled by a cold reservoir through a gas gap. The objective of this paper is to investigate the influence of the eccentricity in the gas gap annulus on the overall heat transfer. For small Biot numbers, temperature gradients in the vial may be neglected and a lumped capacitance assumption is valid. The cooling rate increases as the eccentricity between the two cylindrical surfaces increase. However, when the local Biot number of the vial is large this assumption does not hold. An angular dependence heat transfer model is developed to account for the eccentricity. The model predicted temperature gradients in the vial when the eccentricity is large. Experiments were performed to verify this model. The main conclusion from this study is that eccentricity in the gas gap annulus has a significant effect on the overall heat transfer.

INTRODUCTION

Heat transfer between two surfaces separated by a fluid medium is a common mathematical problem with interest in several applications, namely in gas-gap heat switch, gas bearings, tube-in-tube heat exchangers and many more. The context for our study is a vial, which is a thin-walled cylindrical tube containing a biomedical sample that is cooled in a precooled copper heat sink through a narrow gas gap. We showed that vials cooled using this method have similar cooling speed as quenching in liquid nitrogen [1]. The cold sink is cooled by a cryocooler leading to a sacrificial cryogen free system allowing wider usage of cryogenics in biomedical laboratories. It must be noted that the vials used in clinics vary a lot both the material and the dimensions. Widely used vials are made of either aluminum or polypropylene, which are on the opposite spectrum of the thermal properties.

In case of a closed geometry of a tube placed in a cylindrical hole the effective heat transfer rate increases when the axes of the two objects are not centered. The heat flux between the two objects is a function of the radius of the two cylinders, the degree of eccentricity and the thermal properties of the medium. Analytical expressions are available to completely describe this problem [2]. However, in these models it is assumed that the heat transfer dynamics in the inner tube is fast compared to the heat transfer through the gap medium leading to a constant temperature approximation of the inner tube. This assumption might be acceptable for an aluminum vial because of high thermal diffusivity but is rather questionable for a polypropylene vial. In this paper, we relax this assumption

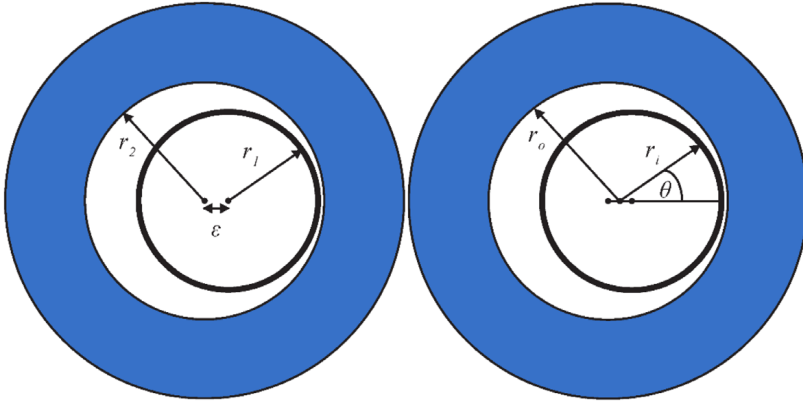


Figure 1. Schematic drawing showing the inner tube and the sink (*left*) and the geometrical representation (*right*)

and consider a case when the heat transfer dynamics in the inner tube is comparable to that through the gap medium. A generalized theoretical model is developed to calculate the overall heat transfer between the inner tube and the sink. This model is validated with experiments.

THEORY

The domain of interest is the region formed by the gap between the inner shell and the outer cylindrical heat sink. We assume here a two-dimensional problem as the length of the cylinders are much larger than the corresponding diameters. The parameters of interest in this study are (see Figure 1):

- Outer radius of the inner cylindrical shell r_1
- Inner radius of the sink r_2
- Thickness of the shell Δr
- Eccentricity ϵ
- Angle θ
- Temperature of the inner cylinder T_v
- Temperature of the heat sink T_c
- Thermal conductivity of the inner cylinder k_v
- Thermal conductivity of the medium in the gap k_g
- Heat capacity of the inner cylinder C

The eccentricity is defined as the distance between the centers of the two cylinders. The maximum value for the eccentricity is equal to $r_1 - r_2$. The distance $r_i(\theta)$ is the distance from the origin to the outer surface of the inner cylindrical shell. The distance $r_o(\theta)$ is the distance from the origin to the inner surface of the heat sink. The angle θ is defined as shown in Figure 1. Therefore, $\theta = 0$ is at the location where the inner cylinder is closest to the heat sink.

Total heat transfer

The steady state heat transfer through such complex geometries can be determined by the graphical analysis [2] where a shape factor S is included in the Fourier equation,

$$Q = k_g S \Delta T = \frac{2\pi k_g L}{\cosh^{-1}\left(\frac{r_1^2 + r_2^2 - \epsilon^2}{2r_1 r_2}\right)} (T_c - T_v)$$

Expressing the shape factor in dimensionless variables: $\eta = r_1/r_2$ and $\xi = \epsilon/r_2$

$$S = \frac{2\pi L}{\cosh^{-1}\left(\frac{\eta^2 - \xi^2 + 1}{2\eta}\right)}$$

When the eccentricity is not equal to zero, one side of the cylindrical shell is closer to the sink than the opposite face, which might lead to different local heat flux. To get an approximation for the heat flux as a function of θ , the following approximation is made,

$$\vec{q}(\theta) = -k_g \Delta T \approx -k_g \frac{\Delta T}{\delta(\theta)} \hat{r}$$

where $\delta(\theta)$ is the distance between the inner cylinder and the heat sink. This distance can be approximated as [3],

$$\delta(\theta) = h_o - \epsilon \cos(\theta)$$

where $h_o = r_2 - r_1$

Therefore, the local heat flux on the surface of the inner cylinder is approximately equal to,

$$\vec{q}(\theta) \approx -k_g \frac{\Delta T}{h_o - \epsilon \cos(\theta)} \hat{r}$$

There are two limiting cases corresponding to the temperature profile in the inner cylindrical shell. First case is when the heat diffusion in the shell is faster than across the medium. The other case is when the heat diffusion in the shell is limited. To express these conditions mathematically we consider the dimensionless Biot number,

$$Bi = \frac{hL}{k}$$

where the h is the heat transfer coefficient to the surroundings, L is the characteristic length, and k is the thermal conductivity of the material.

Figure 2 shows schematically the situation described in this paper, where the heat transfer coefficient is a function of θ . We define a 'local Biot number' with the heat transfer coefficient given by,

$$h = \frac{k_g}{h_o - \epsilon \cos(\theta)}$$

To test for temperature difference between opposite sides of the shell as a characteristic length the diameter ($2r_1$) is considered. The 'local' Biot number Bi_l is,

$$Bi_l = \frac{\left(\frac{2r_1 k_g}{h_o - \epsilon \cos(\theta)}\right)}{k_v} = \frac{2r_1 k_g}{k_v (h_o - \epsilon \cos(\theta))}$$

This local Biot number gives for each value of θ the ratio between the heat flux to the surroundings at that angle and the conduction of heat in the shell. When the Biot number is small, the conduction of heat in the shell is large compared to the heat flux to the surroundings. In other words, the heat

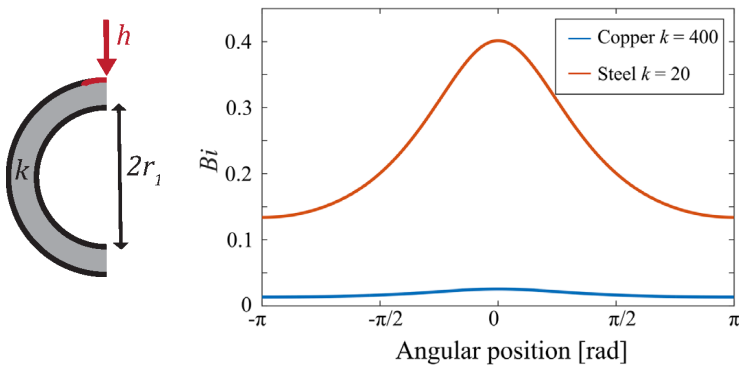


Figure 2. Schematic showing the geometry of the inner tube to define a local Biot number (left) and local Biot number plotted for a Copper and Steel inner tube (right)

conduction from one side to the other in the shell is fast compared to the heat flux to the surroundings. As a result, there is no significant temperature gradient inside the shell and can be treated as a lumped capacitance. When the Biot number is large, the heat conduction in the shell is the same compared to the heat flux to the surroundings leading to temperature gradients inside the shell. For a large local Biot number, modeling the shell as a lumped capacitance is not realistic.

Lumped capacitance

If $Bi_1 \ll 1$ and if $t > (2r_1)^2/\alpha$, with α the thermal diffusivity, one can use the lumped capacitance model,

$$Q = C \frac{dT}{dt} = k_g S \Delta T$$

where C is the capacitance.

The complete differential equation for the lumped capacitance model is

$$\frac{dT}{dt} = \frac{k_g}{C} \frac{2\pi L}{\cosh^{-1}\left(\frac{r_1^2 + r_2^2 - \epsilon^2}{2r_1 r_2}\right)}$$

Angle dependent heat transfer

If $Bi_1 > 1$, it is necessary to divide the cylinder into N elements (at different angles θ_n). Since the wall of the vial is very thin, it is assumed that all the mass is located at the distance r_1 . The heat transfer is assumed only in the θ direction (see Figure 3). For each element the following heat balance holds,

$$q_1 A_1 + (q_{2,right} + q_{2,left}) A_2 = \frac{C}{N} \frac{\partial T_n}{\partial t}$$

where

$$\begin{aligned} q_1(\theta_n) &= k_g \frac{\Delta T_n}{\delta(\theta_n)} = \frac{k_g}{h_o - \epsilon \cos(\theta_n)} (T_c - T_n) \\ A_1 &= L r_1 \Delta \theta \\ q_{2,right} + q_{2,left} &= \frac{k_v}{r_1^2} \frac{\partial^2 T_n}{\partial \theta^2} r_1 \Delta \theta \\ A_2 &= \Delta r \cdot L \end{aligned}$$

The heat equation for one element is

$$\frac{k_g}{h_o - \epsilon \cos(\theta_n)} (T_c - T_n) A_1 + \frac{k_v}{r_1^2} \frac{\partial^2 T_n}{\partial \theta^2} r_1 \Delta \theta A_2 = \frac{C}{N} \frac{\partial T_n}{\partial t}$$

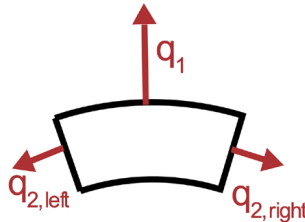
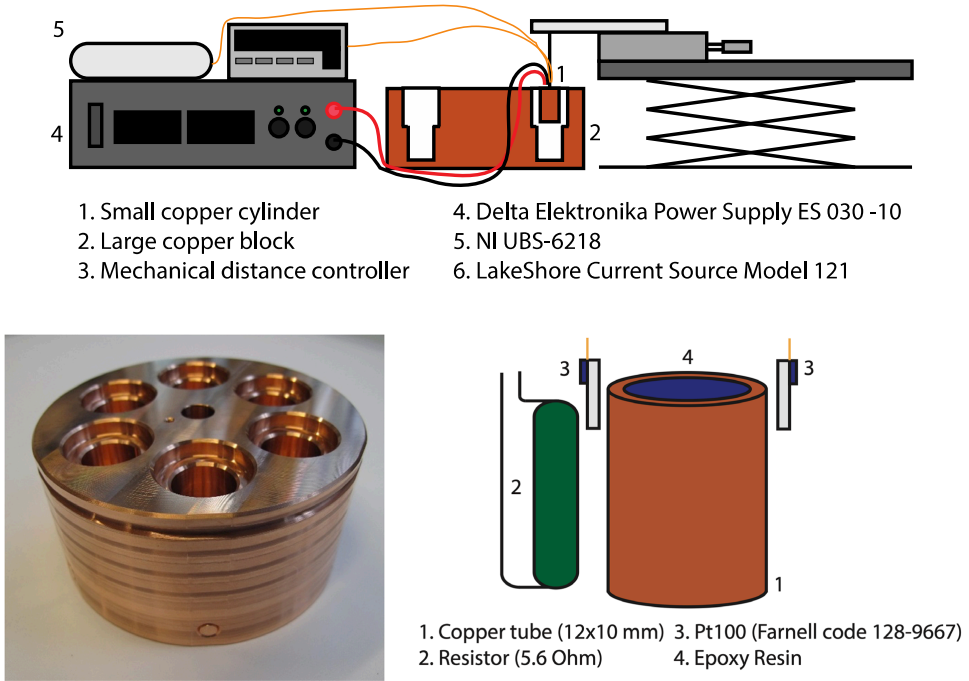


Figure 3. Schematic diagram of one element with the heat flows (heat transfer to the surrounding) and (heat transfer inside the inner tube)



- 1. Small copper cylinder
- 2. Large copper block
- 3. Mechanical distance controller
- 4. Delta Elektronika Power Supply ES 030 -10
- 5. NI UBS-6218
- 6. LakeShore Current Source Model 121

Figure 4. Experimental set up showing the sink and positioning of temperature sensors.

Discretizing this equation using the forward Euler method,

$$T_n^{j+1} = T_n^j \left(1 - 2 \frac{N\Delta t}{C(\Delta\theta)r_1} \frac{k_v}{r_1} A_2 \right) + \frac{N\Delta t}{C(\Delta\theta)r_1} A_2 (T_{n+1}^j + T_{n-1}^j) + \frac{N\Delta t}{C} q_1 A_1$$

EXPERIMENTAL SETUP

Several holes of diameters (16.7, 17.0, 17.4, 17.9 and 18.6 mm) are machined in a copper block. Copper and a stainless steel cylindrical shells are used to simulate different vial materials. Two thermometers are attached on opposite faces of the inner wall of the cylindrical shell and a resistive heater is inserted and is filled with conductive glue to anchor the heater and thermometers. The inner cylinder is positioned in the holes using a mechanical displacement controller with a displacement accuracy of 10 μm. Figure 4 shows a schematic of the experimental test rig. To overcome parasitic losses in the analysis the following methodology is adopted. When a certain heat P is applied the heat balance gives,

$$P = kS(T - T_\infty) + Q'(T) = kS\Delta T + Q'(T)$$

with $Q'(T)$ the parasitic heat leaks that only depend on the temperature T . By keeping T constant and measuring the difference in heating power, the heat losses are eliminated,

$$P_o = kS_o(T - T_\infty) + Q'(T)$$

$$\Delta P = P - P_o = k(S - S_o)(T - T_\infty)$$

where the subscript zero indicates that the measurement was performed when ξ (the eccentricity) was equal to zero. The shape factor S depends on two dimensionless variables: $\xi = e/r_2$ and $\eta = r_1/r_2$, which both can be varied by choosing different holes and the displacement within each hole. In the following section, experimental data are presented.

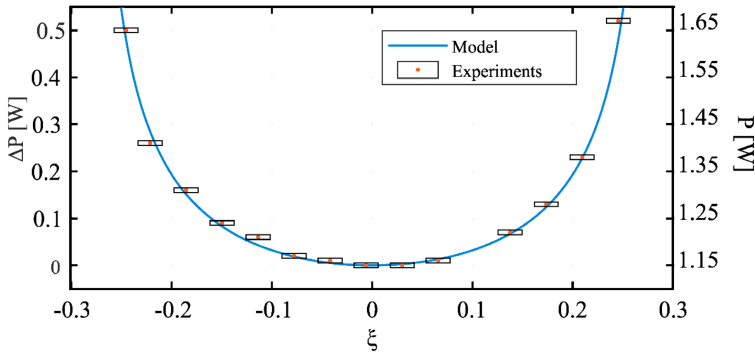


Figure 5. The heating power as a function of ξ (eccentricity).

RESULTS AND DISCUSSION

Steady state experiments

Figure 5 shows the heat applied as a function of eccentricity ξ . The maximum value of ξ in the setup is 0.28. The same figure shows the measured heat, and a fit is made represented by the following equation,

$$P = \frac{2\pi L}{\cosh^{-1}\left(\frac{\eta^2 - ((\xi - a)^2 + b^2)}{2\eta}\right)} k_g \Delta T + c$$

with a , b , and c as fit parameters. Here, a represents an error in the eccentricity positioning, b represents an error in the positioning in the perpendicular direction and c represents an error due to the parasitic heat losses. In Figure 5 the best fit is shown. The following values for the fit parameters were found $a = -0.00126$, $b = 0.03217$, and $c = 0.6861$ W. The fitting parameters a and b can be interpreted as $a \cdot r_2 = -1.054 \times 10^{-5}$ m, $b \cdot r_2 = 2.686 \times 10^{-4}$ m, and $c = 0.6861$ W. In conclusion from the fit, error in the positioning in the eccentricity is around 10 μ m and in the direction perpendicular to the motion 300 μ m. The total heat loss when the temperature difference is 62.3 K is 0.69 W.

Now the experiments are performed in different holes in the copper block to measure the effect of varying η on the heat transfer. The measurement data and the theoretical predictions are shown in Figure 6. Every measurement will probably have a (different) error in ξ , because for every new η (which means another hole with a different diameter) the distance from the edge of the gap has to be calibrated again. This error in eccentricity is estimated to be a maximum value of 0.5 mm. Therefore, the area between the two dotted black lines is the error margin because of the error in ξ . The measurements are in agreement with the overall trend, and they all lie within the error margin.

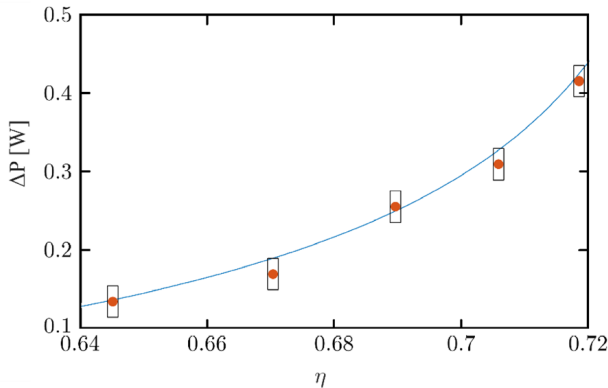


Figure 6. Heating power as a function of η (different sink holes). The eccentricity ξ and the temperature difference ΔT are fixed to a constant value.

During the second experiment ξ was held constant and η was varied. However, keeping ξ constant in every hole of the copper block was difficult, which results in quite a large error margin (see Figure 6). Even though the error margin is large, it can still be clearly seen in the measurements that the power needed to keep the vial at a constant temperature T increase as η increases. Therefore, the heat flow increases as the difference between the radii gets smaller, just like how the shape factor predicts.

Transient experiments

The same test rig used for the steady experiments is also used for transient experiments. The gap between the shell and the sink is filled with water. The rationale for using water is because the thermal conductivity of water is (0.6 W/m•K) is an order of magnitude larger than air (0.025 W/m•K) allowing for testing the case when the Biot number becomes close to one. Additionally, these tests are performed with two types of cylindrical shells, one made of copper as discussed previously and a second made of stainless steel.

Since we expect thermal gradients to be observed in these experiments, let us elaborate further on the location of the temperature sensors in the specimen. When the inner cylinder is eccentrically located in the hole, the largest temperature difference is expected between the side of the shell closest to the heat sink and from the side farthest from the sink (that is between $\theta = 0$ and $\theta = \pi$). The specimen is heated to a certain temperature and then inserted into the hole filled with water and the cooldown process is recorded.

In Figure 7 the results for cooling down the copper cylinder positioned both in the center and eccentrically to the sink are shown. As can be seen in these figures, there is no temperature difference in the copper cylinder in both these cases. For a copper cylinder, there is no temperature gradient inside the material, even when it is not placed in the center. In the same figure the results for cooling down the stainless steel cylinder are shown. In contrast to the results for the copper cylinder, there is a clear difference visible for the stainless steel cylinder between the temperature of both ends if the cylinder is not placed in the center. The temperature of the side of the vial which is closest to the wall ($\theta = 0$) is colder than the other side ($\theta = \pi$). In the beginning the temperature difference is zero, then it rapidly increases and finally it slowly decreases to zero.

The theoretical prediction for the temperatures with time are also shown for both the copper and the stainless steel cylinder. For this theoretical prediction, the heat capacities of the small cylinders were fitted to the measurement data. However, for the stainless steel tube that is eccentrically positioned the theoretical data does not fit well to the experiments. A reason for this might be that some heat is transferred to the epoxy resin. Epoxy resin has a lower thermal conductivity than stainless steel, but over time it might still be conductive enough to cause a deviation from the theoretical model.

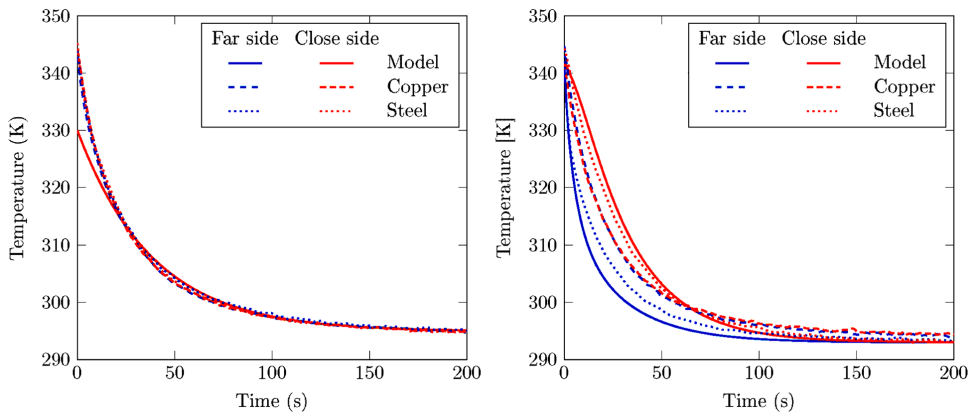


Figure 7. Cooling of a copper and stainless tube in a heat sink without (left) and with (right) eccentricity.

Discussion

Experiments performed on the cooling of an aluminum vial when inserted into a copper sink with a nominal gas-gap of 200 microns are reported in our earlier publication. Since aluminum has a high diffusivity this case can be treated as a lumped capacitance. The model introduced in this paper is applied to this case and the data fit well to the estimations. If a polypropylene vial is used in the snap freezer we expect the misalignment (eccentricity) will cause temperature gradient along the circumference of the vial.

CONCLUSION

A mathematical model is developed to predict the heat transfer between a cylindrical annulus and a heat sink. We show that the total heat transfer depend on the dimension of the wall thickness of the cylinder, the eccentricity, the radius of the annulus and the sink, and thermal properties of the gap medium. We defined a local Biot number to determine the regimes based on this dimensions and geometrical properties. We showed that for low Biot numbers a lumped capacitance approach is suitable. Where as for large Biot numbers thermal gradients will develop along the circumference of the inner cylinder. The model can be used to predict these gradients. Beyond the sacrificial cryogen free tissue snap freezer, the findings reported in this paper will have an impact on the design of cylindrical gas-gap heat switches [4] and tube-in-tube heat exchangers [5].

ACKNOWLEDGMENT

The authors acknowledge the financial support of NWO-TTW under the CryoOn project grant with number 14014.

REFERENCES

1. van Limbeek, M.A., Jagga, J., Holland, H., Ledebuer, K., ter Brake, M., Vanapalli, V., "Cooling of a vial in a snapfreezing device without using sacrificial cryogens," *Sci Rep*, 9(1) (2019), pp. 1-9.
2. Bergman, T.L., Bergman, T.L., Incropera, F.P., Dewitt, D.P., Lavine, A.S., *Fundamentals of heat and mass transfer*, John Wiley & Sons, (2011).
3. Ming, C., Li-li, C., "Analysis of the eccentric cylindrical thin shell," *Applied Mathematics and Mechanics*, 15(9), (1994), pp. 887-895.
4. DiPirro, M. J., Shirron, E. P., "Heat switches for ADRs," *Cryogenics*, 62, (2014), pp. 172-176.
5. Fan, M., Bao, Z., Liu, S., Huang, W., "Flow and heat transfer in the eccentric annulus of the helically coiled tube-in-tube heat exchanger used in an aero-engine," *International Journal of Thermal Sciences*, 179, (2022), p. 107636.